AD-A048 851 JOHNS HOPKINS UNIV LAUREL MD APPLIED PHYSICS LAB F/G 4/1
THE SEMIANNUAL VARIATION IN THE UPPER ATMOSPHERE (900-1200 KM) --ETC(U)
SEP 77 A EISNER, S M YIONOULIS N00017-72-C-4401
UNCLASSIFIED APL/JHU/TG-1314 NL

| OF |
AD A048851

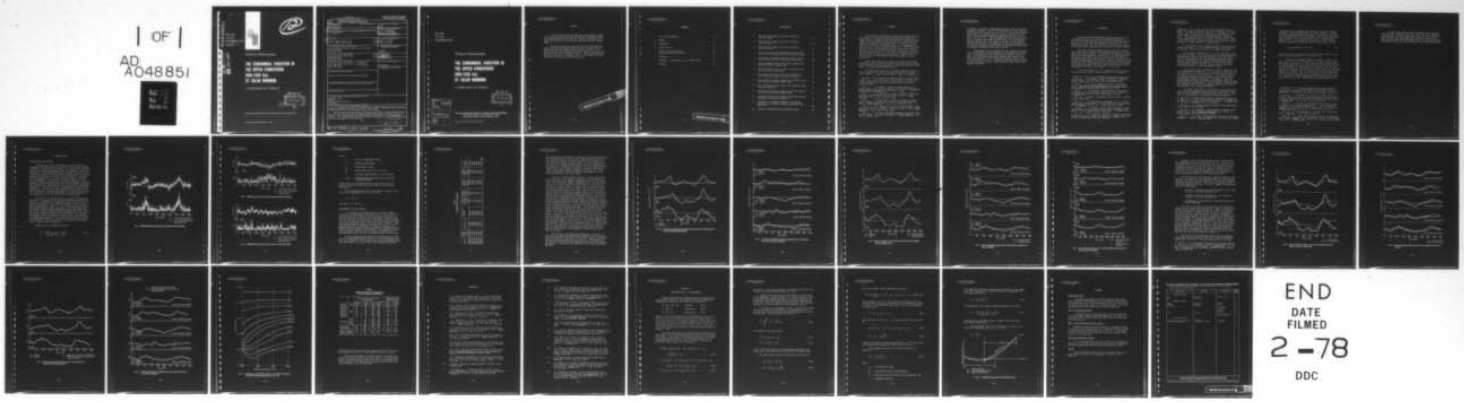

END
DATE FILMED
2-78
DDC

APL/JHU
TG 1314
SEPTEMBER 1977
Copy No. 2

12
B.S.

Technical Memorandum

THE SEMIANNUAL VARIATION IN THE UPPER ATMOSPHERE (900-1200 km) AT SOLAR MINIMUM

A. EISNER AND S. M. YIONOULIS

THE JOHNS HOPKINS UNIVERSITY ■ APPLIED PHYSICS LABORATORY

Unclassified

SECURITY CLASSIFICATION OF THIS PAGE

PLEASE FOLD BACK IF NOT NEEDED FOR BIBLIOGRAPHIC PURPOSES

REPORT DOCUMENTATION PAGE

1. REPORT NUMBER	2. GOVT ACCESSION NO	3. RECIPIENT'S CATALOG NUMBER
APL/JHU/TG-1314		

4. TITLE (and Subtitle)
THE SEMIANNUAL VARIATION IN THE UPPER ATMOSPHERE (900-1200 km) AT SOLAR MINIMUM

5. TYPE OF REPORT & PERIOD COVERED
Technical Memorandum
1974-1976

6. PERFORMING ORG. REPORT NUMBER

7. AUTHOR(s)
A. Eisner and S. M. Yionoulis

8. CONTRACT OR GRANT NUMBER(s)
N0017-72-C-4401

9. PERFORMING ORGANIZATION NAME & ADDRESS
The Johns Hopkins University Applied Physics Laboratory
Johns Hopkins Rd.
Laurel, MD 20810

10. PROGRAM ELEMENT, PROJECT, TASK AREA & WORK UNIT NUMBERS
Task S1LO

11. CONTROLLING OFFICE NAME & ADDRESS
Naval Plant Representative Office
Johns Hopkins Rd.
Laural, MD 20810

12. REPORT DATE
September 1977

13. NUMBER OF PAGES
37

14. MONITORING AGENCY NAME & ADDRESS
Naval Plant Representative Office
Johns Hopkins Rd.
Laurel, MD 20810

37p.

15. SECURITY CLASS. (of this report)
Unclassified

15a. DECLASSIFICATION/DOWNGRADING SCHEDULE

16. DISTRIBUTION STATEMENT (of this Report)
Approved for public release; distribution unlimited.

17. DISTRIBUTION STATEMENT (of the abstract entered in Block 20, if different from Report)

18. SUPPLEMENTARY NOTES

19. KEY WORDS (Continue on reverse side if necessary and identify by block number)
atmospheric density
NNSS data
semiannual density variation
Transit data

20. ABSTRACT (Continue on reverse side if necessary and identify by block number)

A new method has been developed that uses satellite along-track position errors to obtain information on atmospheric densities at altitudes of 900 to 1200 km. The data base used was the daily tracking results from the Navy Navigation Satellite System (NNSS).

Densities derived from these data (for the years 1974-76) show a pronounced semiannual variation, with the April/October maxima exceeding the August/January minima by factors of 2 to 4. The variation is more pronounced than was previously reported, and double the best current modeled variation. The current resolution with this technique is estimated to be 1×10^{-19} gm/cm^3, or about 10% of the total density at these altitudes.

10 to the -19th power gm/cu cm

DD FORM 1 JAN 73 1473 031 650

Unclassified

SECURITY CLASSIFICATION OF THIS PAGE

APL/JHU
TG 1314
SEPTEMBER 1977

Technical Memorandum

THE SEMIANNUAL VARIATION IN THE UPPER ATMOSPHERE (900-1200 km) AT SOLAR MINIMUM

A. EISNER AND S. M. YIONOULIS

THE JOHNS HOPKINS UNIVERSITY ■ APPLIED PHYSICS LABORATORY
Johns Hopkins Road, Laurel, Maryland 20810
Operating under Contract N00017-72-C-4401 with the Department of the Navy

THE JOHNS HOPKINS UNIVERSITY
APPLIED PHYSICS LABORATORY
LAUREL MARYLAND

ABSTRACT

A new method has been developed that uses satellite along-track position errors to obtain information on atmospheric densities at altitudes of 900 to 1200 km. The data base used was the daily tracking results from the Navy Navigation Satellite System (NNSS).

Densities derived from these data (for the years 1974-76) show a pronounced semiannual variation, with the April/October maxima exceeding the August/January minima by factors of 2 to 4. The variation is more pronounced than was previously reported, and double the best current modeled variation. The current resolution with this technique is estimated to be 1×10^{-19} gm/cm^3, or about 10% of the total density at these altitudes.

CONTENTS

ILLUSTRATIONS

1. SUMMARY

We have devised a method that employs the along-track position errors of a satellite system to correct the Jacchia air-density model. We have used the Navy Navigation Satellite System (NNSS, or Transit System), which consists of a constellation of satellites in near-circular polar orbits at altitudes of 900 to 1200 km. The satellite along-track error is very sensitive to drag errors; an error in the mean density of 2×10^{-19} gm/cm^3 will result in a day in an along-track error that will grow quadratically to 14 m. This is easily detectable with present satellite-position precision (Ref. 1). From these considerations we estimate that the resolution with the technique (using 1-day averages) is about 1×10^{-19} gm/cm^3 (10% of the density at these altitudes).

Using the new method, we analyzed the data from six NNSS satellites. Daily values of satellite along-track position errors were converted to daily mean-density corrections, which were then added to the mean modeled density (Ref. 2).

The semiannual variation in the upper atmosphere density is clearly evident in the data. Our results confirm the earlier Echo 2 (Refs. 3, 4, and 5) and Calsphere-1 (Ref. 6) findings that

---

Ref. 1. H. D. Black, R. E. Jenkins, and L. L. Pryor, "The Transit System, 1975," APL/JHU TG 1305, December 1976 (also presented at the 56th Annual American Geophysical Union Meeting, 16-20 June 1975).

Ref. 2. L. G. Jacchia, "Static Diffusion Models of the Upper Atmosphere with Empirical Temperature Profiles," Smithsonian Contribution to Astrophysics, Vol. 8, No. 9, 1965.

Ref. 3. G. E. Cook and D. W. Scott, "Exospheric Densities Near Solar Minimum Derived from the Orbit of Echo-2," Planet. Space Sci., Vol. 14, pp. 1149-1165, 1966.

Ref. 4. G. E. Cook and D. W. Scott, "Variations in Exospheric Density at Heights Near 1100 km, Derived from Satellite Orbits," Planet. Space. Sci., Vol. 15, pp. 1933-1956, 1967.

Ref. 5. G. E. Cook and D. W. Scott, "The Semi-Annual Variation on Air Density at Height of 1100 km from 1964 to 1967," Planet. Space Sci., Vol. 17, pp. 107-119, 1969.

Ref. 6. G. E. Cook, "The Large Semi-Annual Variation in Exospheric Density: A Possible Explanation," Planet. Space Sci., Vol. 15, pp. 627-632, 1967.

the density at heights of approximately 1000 km shows a pronounced semiannual variation. The 1976 data indicate an October maximum exceeding the July minimum by a factor of 2.5 and an April maximum nearly double the January minimum. Satellite 1973-81a for the years 1974-1976 shows an October maximum exceeding the July minimum by a factor of 3.6. The discrepancy may be accounted for, in part, by changing the modeled diurnal effect. We also observed the existence of local July maxima in the data from satellites 1973-81a and 1970-67a. The maxima may be partly accounted for by an error in the amplitude and/or phase of the diurnal bulge and/or the seasonal-latitudinal variations of helium.

Improvements in gravity models are also possible with satellites in near resonance with harmonics in the geopotential expansion. For example, the data from satellite 1967-34a clearly exhibit a 28-day resonant oscillation arising from errors in the 27th-order harmonics. Future NNSS satellites may exhibit other strong resonances as well. If unexpected resonance effects appear we also would have to remove these, possibly to get access to the density variations.

2. BACKGROUND

During the period 1958-1963 we worked intensively on the analysis and software for the Navy Navigation System (Ref. 7). Our effort was concerned mostly with the orbit determination programs that are used daily in computing the ephemerides of the Transit satellites. The five satellites are all in polar orbits at different nodal longitudes and at altitudes of 950 to 1200 km.

Since 1963, when the program became operational, APL has been responsible for updating and improving the precision of the system via software changes. Our efforts (of geophysical significance) have concentrated on the following: (a) improvements in the geopotential model of the earth including the discovery of "resonant" geopotential effects (Refs. 8 and 9), a revision of the Jacchia air-density model to adapt it to the above-800-km altitude regime (Ref. 10), an implementation of polar motion in the ephemeris construction (Ref. 11), and construction of a model of the tropospheric refraction effect (Refs. 7, 12, and 13).

The data we have used in our air-density studies are the normal day-to-day quality control statistic on the ephemeris

---

Ref. 7. H. D. Black, "Position Determination Using the Transit System," International Geodetic Symposium on Satellite Doppler Positioning, Las Cruces, NM, 12-14 October 1976.

Ref. 8. W. H. Guier, "Geodetic Problems and Satellite Orbits," Lectures in Applied Mathematics, Vol. 6, Space Mathematics, Part II, American Mathematical Society, 1966.

Ref. 9. S. M. Yionoulis, "Determination of Coefficients Associated with the Geopotential Harmonics of Order Thirteen," J. Geophys. Res., Vol. 71, No. 6, March 1966, p. 1768.

Ref. 10. A. Eisner, "Atmospheric Density Studies," APL/JHU TG 951, December 1967.

Ref. 11. V. L. Pisacane, B. B. Holland, and H. D. Black, "Recent (1973) Improvements in the Navy Navigation Satellite System," Navigation, Vol. 20, No. 3, Fall 1973, pp. 224-229.

Ref. 12. H. S. Hopfield, "Two-Quartic Tropospheric Refractivity Profile for Correcting Satellite Data," J. Geophys. Res., Vol. 74, No. 18, August 1969, pp. 4487-4499.

Ref. 13. S. M. Yionoulis, "Algorithm to Compute Tropospheric Refraction Effects on Range Measurements," J. Geophys. Res., Vol. 75, No. 36, 20 December 1970, pp. 7636-7637.

production. Prior to 1967, we had used the Harris-Priester model of the upper air density (Ref. 14) in computing the ephemerides. The rising solar cycle forced us to implement the newer Jacchia model in hopes that it would diminish the ephemeris error. (The normal operation of Transit requires a prediction of the satellite position 12 to 24 hours into the future. Errors in the density model cause period errors in the satellite ephemeris that, if large enough, can be catastrophic.)

We implemented a strict interpretation of the Jacchia air-density model (Ref. 2) in the ephemeris complex, realizing that no data above 800 km had been used in the model development.

We attempted to implement it in the daily satellite operations but it failed. We later learned that we had attempted the implementation during a very severe magnetic storm (May 1967). An intensive investigation (Ref. 10) showed that the model consistently overestimated the air density during disturbed magnetic periods. Minor parameter adjustments to the basically sound Jacchia model solved the problem. We have used it ever since with daily insertion of solar and magnetic indexes.

About 18 months ago, we shifted the Transit system from the APL 4.5 geopotential model (Ref. 15) to the WGS-72 model (Ref. 16). For some time prior to this we had noticed an apparent anomaly in the results from one of the satellites. Of the five satellites, the anomalous-behaving satellite had the lowest perigee height. We had sought in vain for the cause of the anomaly. When the anomaly persisted after the change in geopotential models, we seriously suspected the drag model. One of us (Eisner) remembered that the semiannual term in the Jacchia model phase-matched our data; this was the key to resolving the problem.

The Jacchia model (Ref. 2) incorporated a semiannual variation in the mean exospheric temperature with an amplitude proportional to the average 10.7-cm solar radiation flux, $\bar{F}_{10.7}$. Cook (Ref. 17) found that the Jacchia model under-represents the

---

Ref. 14. I. Harris and W. Priester, "Theoretical Models for the Solar-Cycle Variation of the Upper Atmosphere," J. Geophys. Res., Vol. 67, No. 12, November 1962, pp. 4585-4591.

Ref. 15. H. D. Black, "Doppler Tracking of Near-Earth Satellites," APL/JHU TG 1031, 1968.

Ref. 16. T. O. Seppelin, "The Department of Defense World Geodetic System 1972," The Canadian Surveyor, Vol. 28, No. 5, Ottawa, Canada, December 1974, pp. 496-506.

Ref. 17. G. E. Cook, "The Semi-Annual Variation in the Upper Atmosphere: A Review," Ann. de Geophys., Vol. 25, 1969, pp. 451-469.

semiannual effect at heights above 1000 km, a conclusion that was confirmed in our investigations of the NNSS satellites. Jacchia (Ref. 18) acknowledged the shortcomings of the earlier model and switched from a solar-activity-dependent effect (caused by temperature variations) to a functional form that is strongly height-dependent but is independent of solar activity. In his latest model he expresses the semiannual density variation in the form

$$\Delta \log_{10}(\text{semiannual}) = f(z)\, g(t) \ , \qquad (1)$$

where f(z) relates the amplitude to height and g(t) represents the average density variations as a function of time.

Helium is the dominant component at 1000 km. Hedin et al. (Ref. 19) found a morning maximum for helium located in the winter hemisphere. Von Zahn et al. (Ref. 20) emphasize the dominance of the annual migration of the helium bulge over the diurnal variation and the difficulty of separating the two effects. The so-called "winter helium bulge," first discovered in 1967 (Ref. 21), was later shown to be a special case of the more general seasonal-latitudinal variation in density. Mayr and Volland (Ref. 22) concluded from all the available evidence that the semiannual effect consists of two components (a global component and a latitude-dependent component), both of which are associated with temperature variations.

Ref. 18. L. G. Jacchia, "Revised Static Models of the Thermosphere and Exosphere with Empirical Temperature Profiles," Smithsonian Astrophysical Observatory Special Report 332, May 1971.

Ref. 19. A. E. Hedin, H. G. Mayr, C. A. Reber, and N. W. Spencer, "Empirical Model of Global Thermospheric Temperature and Composition Based on Data from OGO-6, Quadrapole Mass Spectrometer," J. Geophys. Res., Vol. 70, No. 1, 1975, pp. 215-225.

Ref. 20. V. Von Zahn, W. Köehnleon, K. H. Fricke, V. Laux, H. Trinds, and H. Volland, "ESRO 4 Model of Global Thermospheric Composition and Temperatures During Times of Low Solar Activity," Geophys. Res. Lett., Vol. 4, No. 1, January 1977, pp. 34-36.

Ref. 21. G. M. Keating and E. J. Prior, "The Winter Helium Bulge," Space Res., Vol. 8, 1968, pp. 982-992.

Ref. 22. H. G. Mayr and H. Volland, "Theoretical Model for the Latitude Dependence of the Thermospheric Annual and Semi-Annual Variations," J. Geophys. Res., Vol. 77, No. 34, 1972, pp. 6774-6790.

Jacchia's 1965 model was heavily weighted toward the lower regions of the atmosphere since few, if any, data were available above 1000 km. Jacchia's latest model (Ref. 18) has incorporated data from the Echo-2 and Calsphere-1 satellites together with seasonal-latitudinal helium variations (Ref. 21), thereby extending the model well into the altitude regime of the Transit satellites.

3. CURRENT STATUS

SATELLITE DATA DESCRIPTION

Each satellite in the constellation of polar satellites transmits its current position in addition to the doppler carriers (a frequency pair at 150 and 400 MHz). The position is a real-time readout from a predicted ephemeris that is contained in the satellite memory. The predicted ephemeris is generated as follows. On a continuing basis, a network of ground stations takes all possible doppler data from passes (transits) of the satellites. The data are then transmitted to a central processing center. There they are accumulated into 36-hour spans for each satellite. A least-squares estimation is performed on each span to determine a set of satellite initial conditions that, when used to generate the satellite ephemeris, gives the best fit to the doppler data. (Numerical integration of the forces acting on the satellite is used for this computation.) The set of initial conditions is then used to predict the satellite ephemeris approximately 30 hours beyond the end of the data span. The predicted ephemeris is then transmitted to the satellite, where it is stored in the satellite memory.

The input or "starting" orbit for a current 36-hour span is obtained by re-epoching the orbit determined from the previous 36-hour span. An analysis of the doppler residuals over the new span measures the quality of the predicted ephemeris currently being used in the satellite. The rms of the residuals, T (in meters), is plotted versus time in Figs. 1, 2, and 3. The changes in initial conditions obtained in the estimation procedure also reflect how the accuracy of the predicted ephemeris degrades with time. One of the initial-condition parameters is highly sensitive to secular or long-period errors in the satellite-motion model. The parameter is routinely plotted to provide a "quick-look" estimate of the predicted-ephemeris precision. It provides an excellent data source for studying the long-term behavior of atmospheric density model errors. This is shown in Appendix A.

From Eq. A-12 of Appendix A we obtain

$$\delta\rho = -\frac{2}{3}\left[\frac{n}{C_d \frac{A}{M} V^2 (t_1 - t_0)}\right] A_1 , \qquad \text{(A-12)}$$

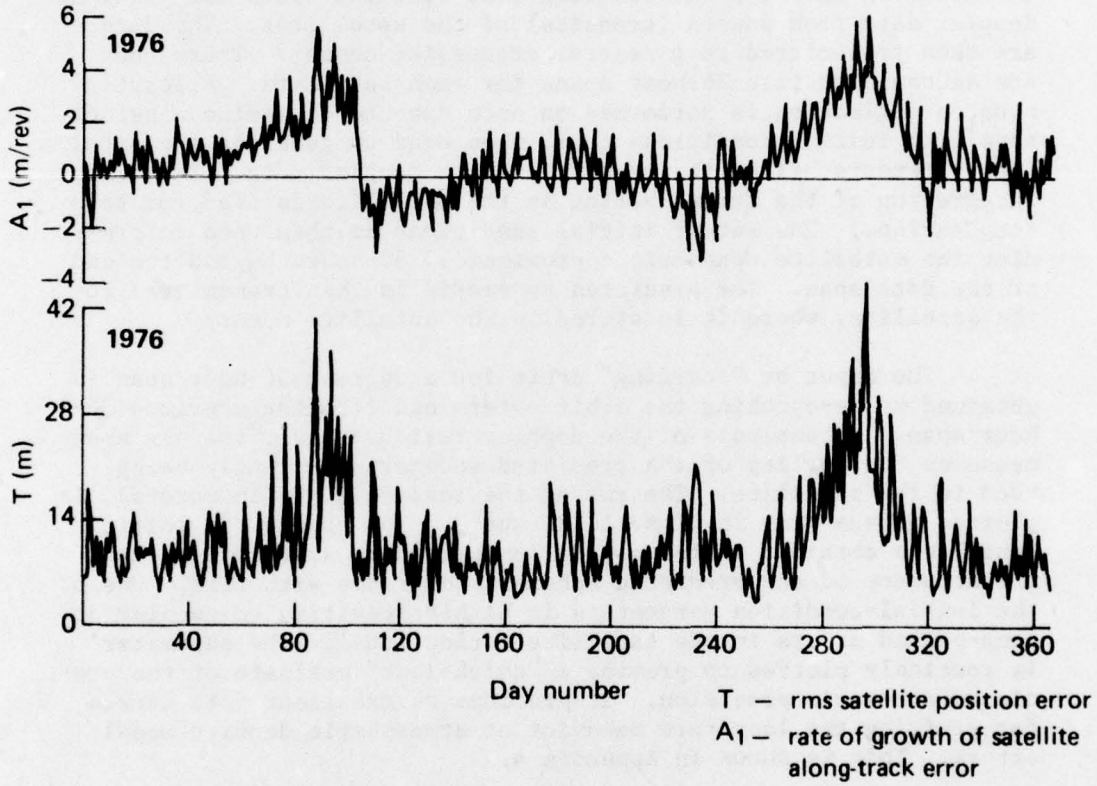

Fig. 1 NNSS Satellite Summary Statistics, Satellite 1973-81a (30200)

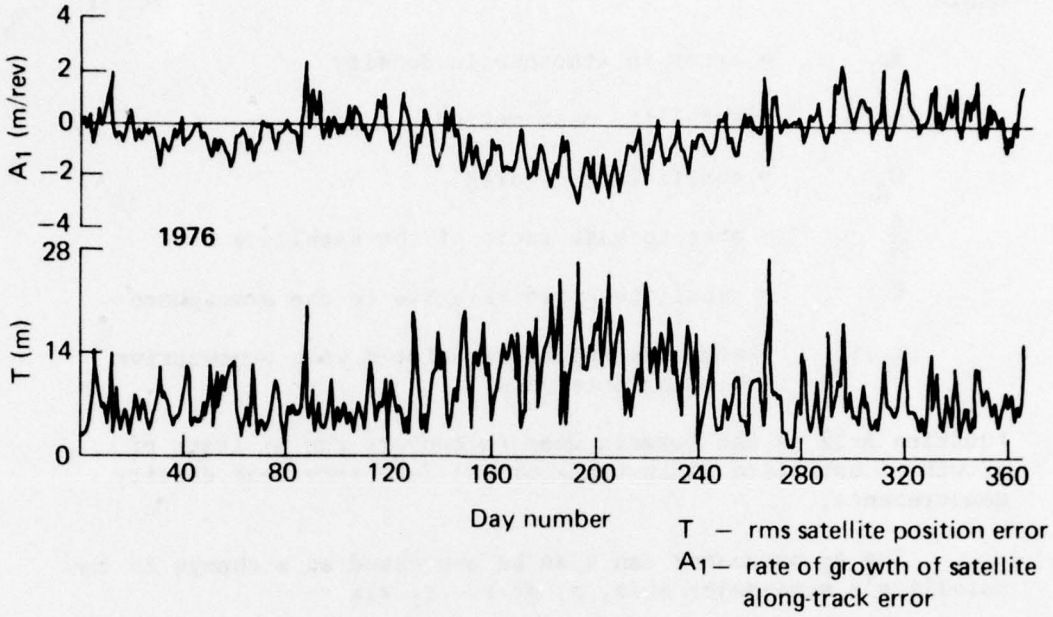

Fig. 2 NNSS Satellite Summary Statistics, Satellite 1967-92a (30140)

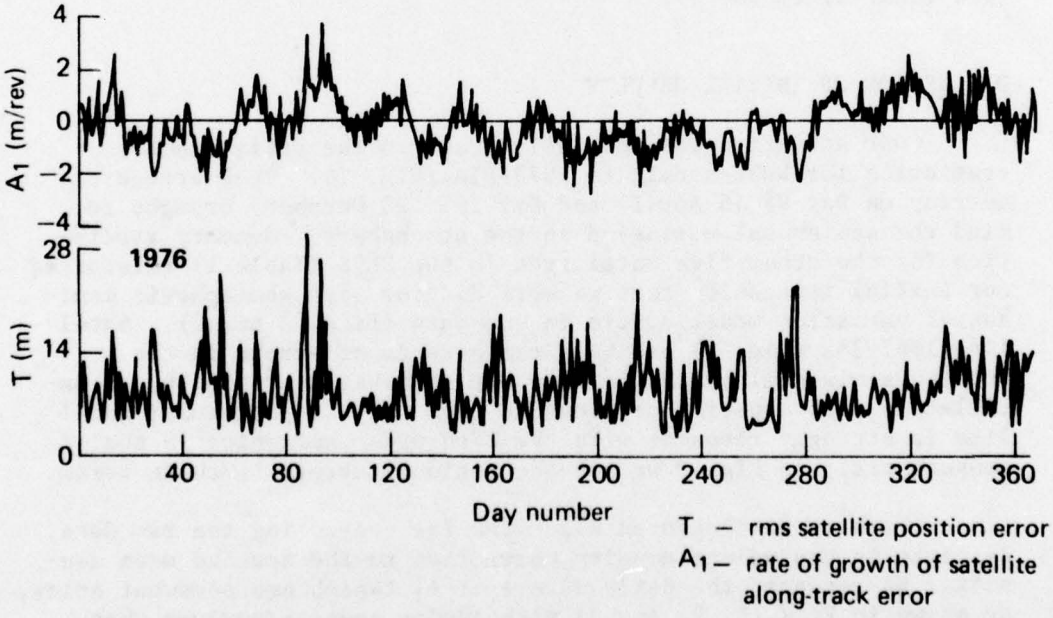

Fig. 3 NNSS Satellite Summary Statistics, Satellite 1967-34a (30120)

where

$\delta\rho$ = error in atmospheric density

n = satellite mean motion

C_d = coefficient of drag

$\frac{A}{M}$ = area-to-mass ratio of the satellite

V = satellite speed relative to the atmosphere

t_0, t_1 = starting epochs associated with consecutive fitting intervals

Equation A-12 is the formula used to convert the A_1 (rate of growth of satellite along-track error) data into mean density measurements.

The A_1 parameter can also be expressed as a change in the satellite's semi-major axis, a, at $t = t_1$ via

$$A_1 = -\frac{3}{2}\,\delta a$$

(see Figs. 1, 2, and 3).

DISCUSSION OF INITIAL RESULTS

Our attention was initially drawn to the daily summary statistics for NNSS satellite 1973-81a (Fig. 1). Peak errors occurring on Day 95 (6 April) and Day 295 (23 October) brought to mind the semiannual variation in the atmosphere. Summary statistics for the other five satellites in the NNSS (Table 1) reinforced our initial impression that we were dealing with atmospheric semiannual variation model errors in the data (Figs. 2 and 3). Satellite 1967-34a (Fig. 3) exhibits the effects of errors in the modeled semiannual variation that are somewhat corrupted by an oscillation with a period of about 28 days. (This particular satellite is strongly resonant with the 27th-order harmonics in the geopotential; in Fig. 3 we see the residual errors in these terms.

We have developed an algorithm for converting the raw data, A_1, into an equivalent density correction to the modeled mean density. We replaced the daily values of A_1 (which are somewhat noisy, as shown in Figs. 1, 2, and 3) with 10-day averaged values that

Table 1

Satellites Used in the Study

Satellite	Semi-Major Axis (km)	Eccentricity	Inclination (deg)	Nodal Position 1 Jan 76 (deg)	Perigee Position 1 Jan 76 (deg)	Nodal Precession Rate (deg/day)	Perigee Precession Rate (deg/day)	Years Covered
1967-34a	7449	0.002	90.20	23	180	0.021	−2.90	1976
1967-48a	7463	0.002	89.60	− 47	133	−0.038	−2.86	1976
1967-92a	7454	0.005	89.25	− 35	119	−0.077	−2.87	1976
1968-12a	7462	0.008	89.98	− 84	294	−0.002	−2.87	1976
1970-67a	7464	0.018	90.10	−109	37	−0.009	−2.85	1976
1973-81a	7399	0.017	90.16	123	131	−0.019	−2.97	1974-1976

are well-suited to the study of a variation having a 180-day period. The resulting density corrections for satellite 1973-81a for the years 1974-1976 and for the other five NNSS satellites for the year 1976 are presented in Figs. 4 and 5. We then added the corrections to the modeled mean densities (used in the generation of the ephemeris). Figures 6 and 7 present the actual mean densities experienced by the six NNSS satellites. Satellite 1973-81a exhibits a pronounced semiannual variation throughout the period studied (1974-1976). There is generally good agreement in both phase and amplitude from year to year.

We note a curious peaking in density in July, particularly in the 1976 data. The peaking is partially accounted for by the diurnal bulge "beating" against perigee position: The NNSS satellites have nearly polar orbits; consequently their orbital planes precess very slowly in inertial space (Table 1). Since the sun and bulge move about 1°/day, it follows that the satellite plane contains the diurnal bulge twice yearly (once each on the ascending and descending nodes of the orbit). The net effect is very small unless the eccentricity is large enough for the position of perigee relative to the diurnal bulge to play a part. The diurnal and semiannual variations for 1973-81a and 1970-67a (the two relatively eccentric NNSS satellites) interfere constructively (or destructively) resulting in the appearance of an enhanced (or suppressed) pseudosemiannual variation. Satellite 1973-81a is particularly interesting (Fig. 8). At the start of 1976, perigee (located on the ascending-node side of the orbit) moves through the diurnal bulge, resulting in peak mean densities. One hundred eighty days later, perigee has precessed 540° and is once again traversing through the diurnal bulge (on the descending-node side of the orbit). The cycle is completed 180 days later (at the end of 1976) when the situation is the same as it was at the start of 1976. This pattern is repeated over several years because of the very small nodal precession rate of 1973-81a and the fact that perigee returns to its starting position every 365 days. The peaking densities at the beginning, middle, and end of the year due to the diurnal bulge destructively interfere with the semiannual minima occurring approximately at the same times. The result is particularly evident in July and August where an expected minimum (particularly in 1976 data) is replaced with a local maximum. We will discuss this in more detail later.

In addition to the semiannual and diurnal variations, we also have to contend with the seasonal variations in the concentration of helium (Refs. 20 and 21). This effect results in peak densities occurring in January and July (Fig. 8). These maxima destructively interfere with the semiannual minima occurring at about the same time, resulting in the appearance of a reduced semiannual amplitude.

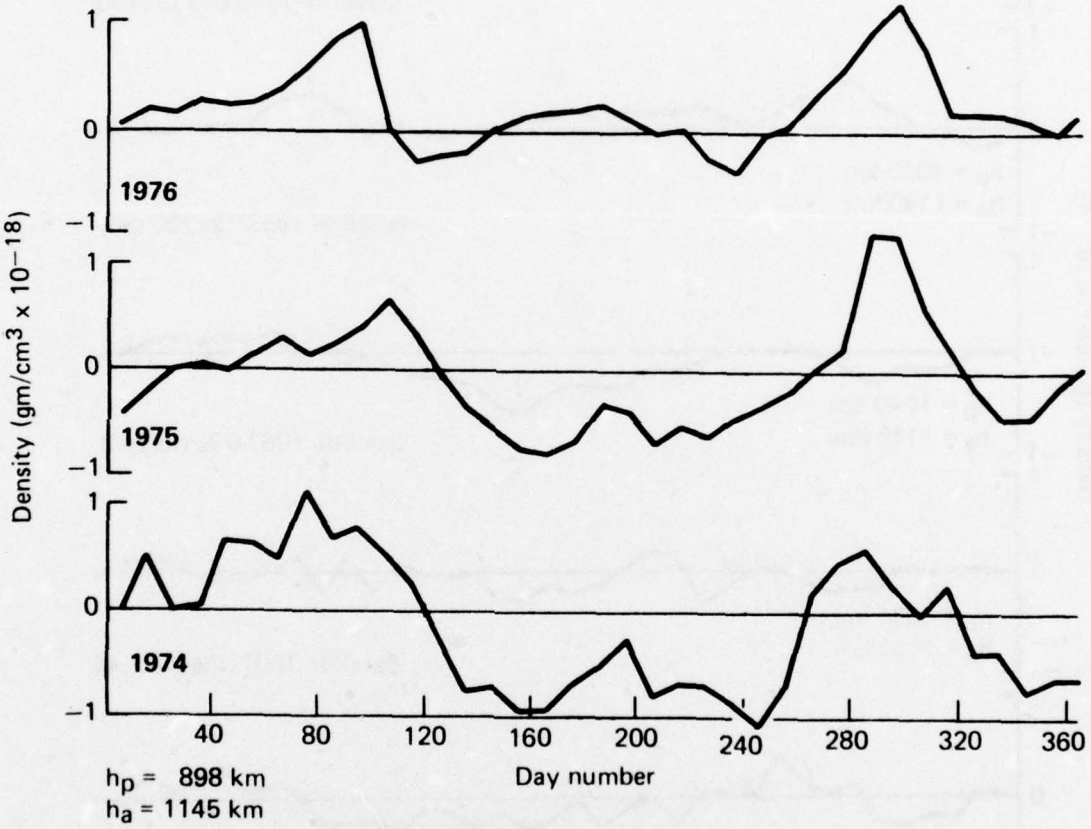

Fig. 4 Corrections to Modeled Atmospheric Density versus Time (derived from Satellite 1973-81a (30200) data)

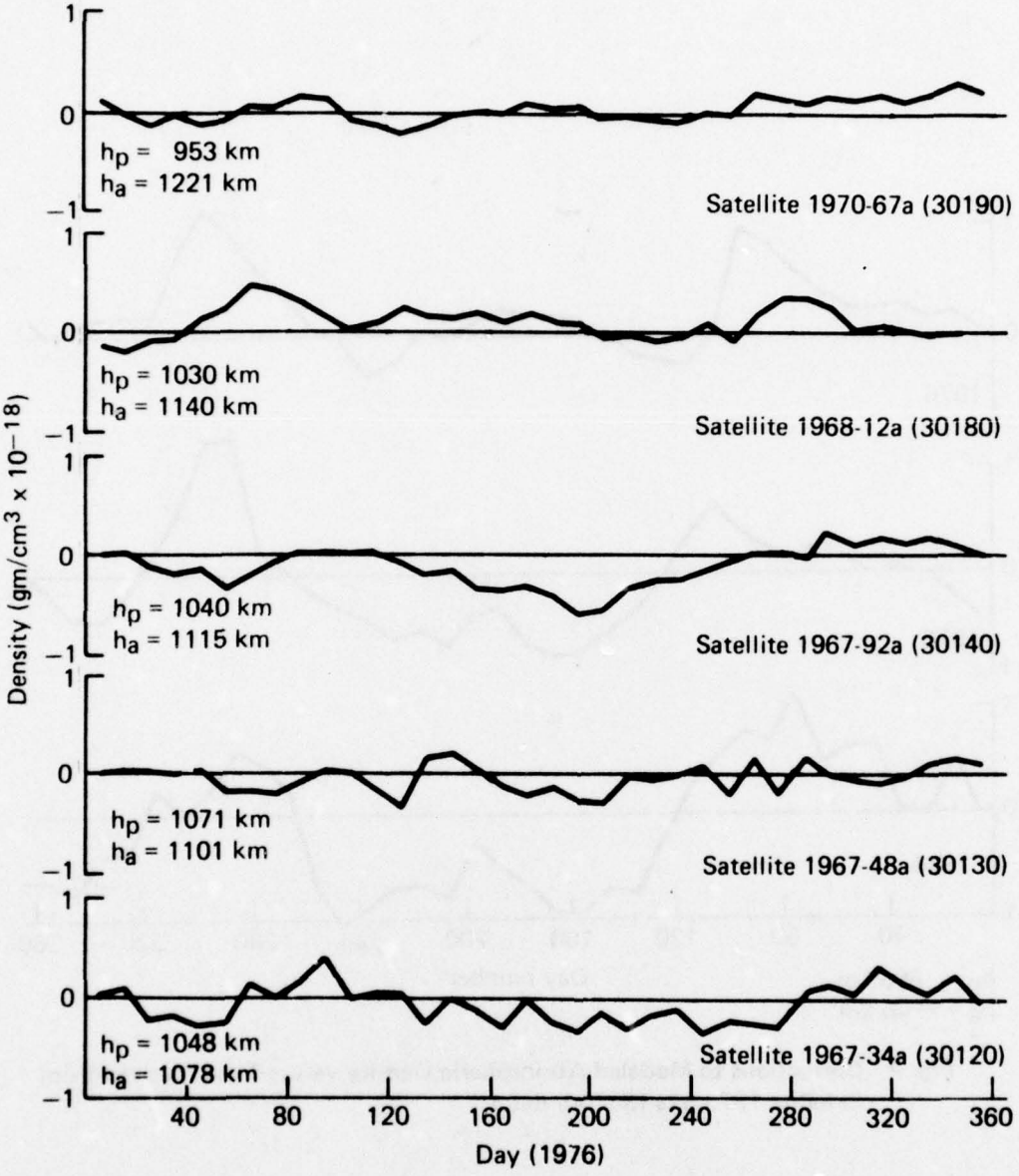

Fig. 5 Corrections to Modeled Atmospheric Density versus Time (derived from data from various satellites)

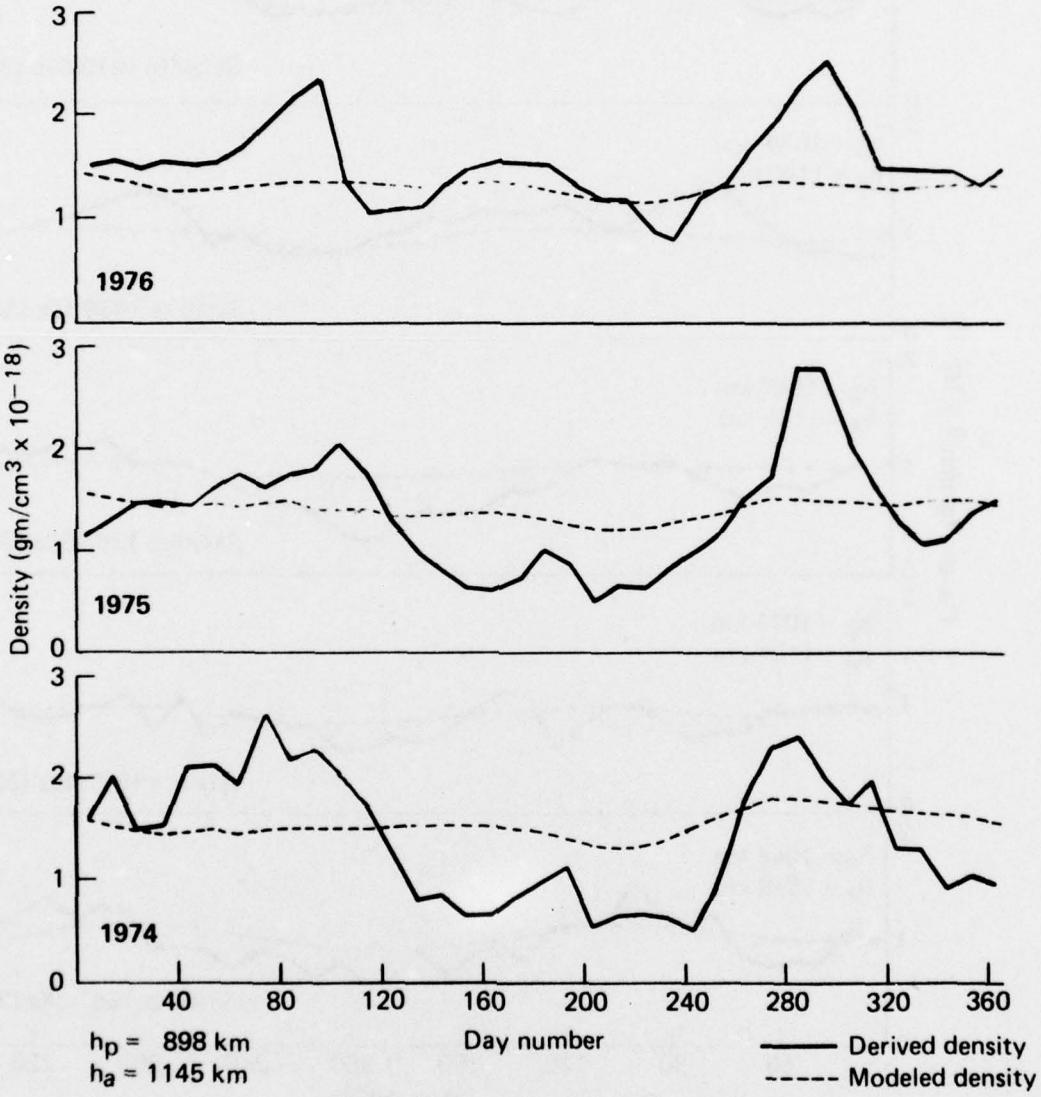

Fig. 6 Mean Atmospheric Density versus Time (derived from Satellite 1973-81a (30200) data)

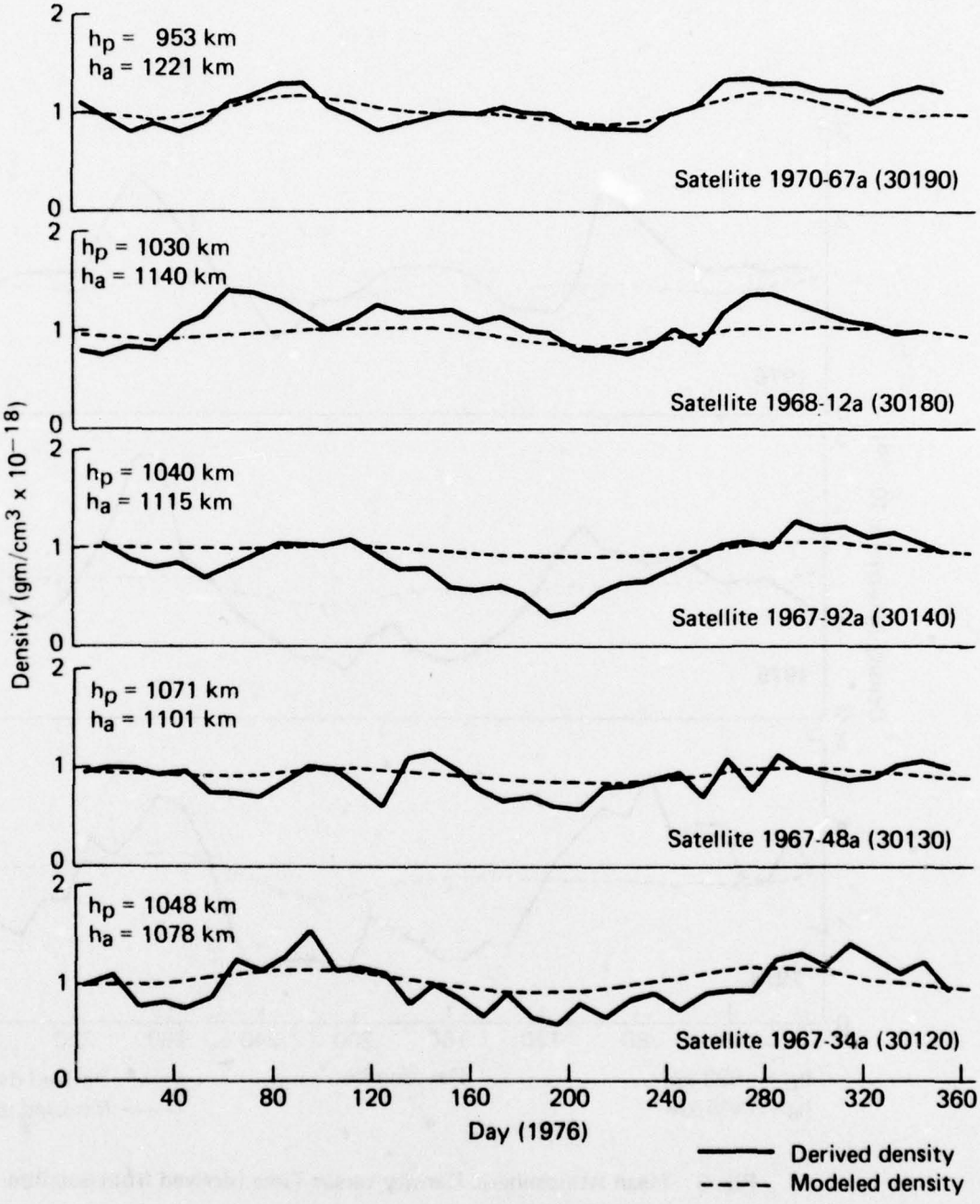

Fig. 7 Mean Atmospheric Density versus Time (derived from data from various satellites)

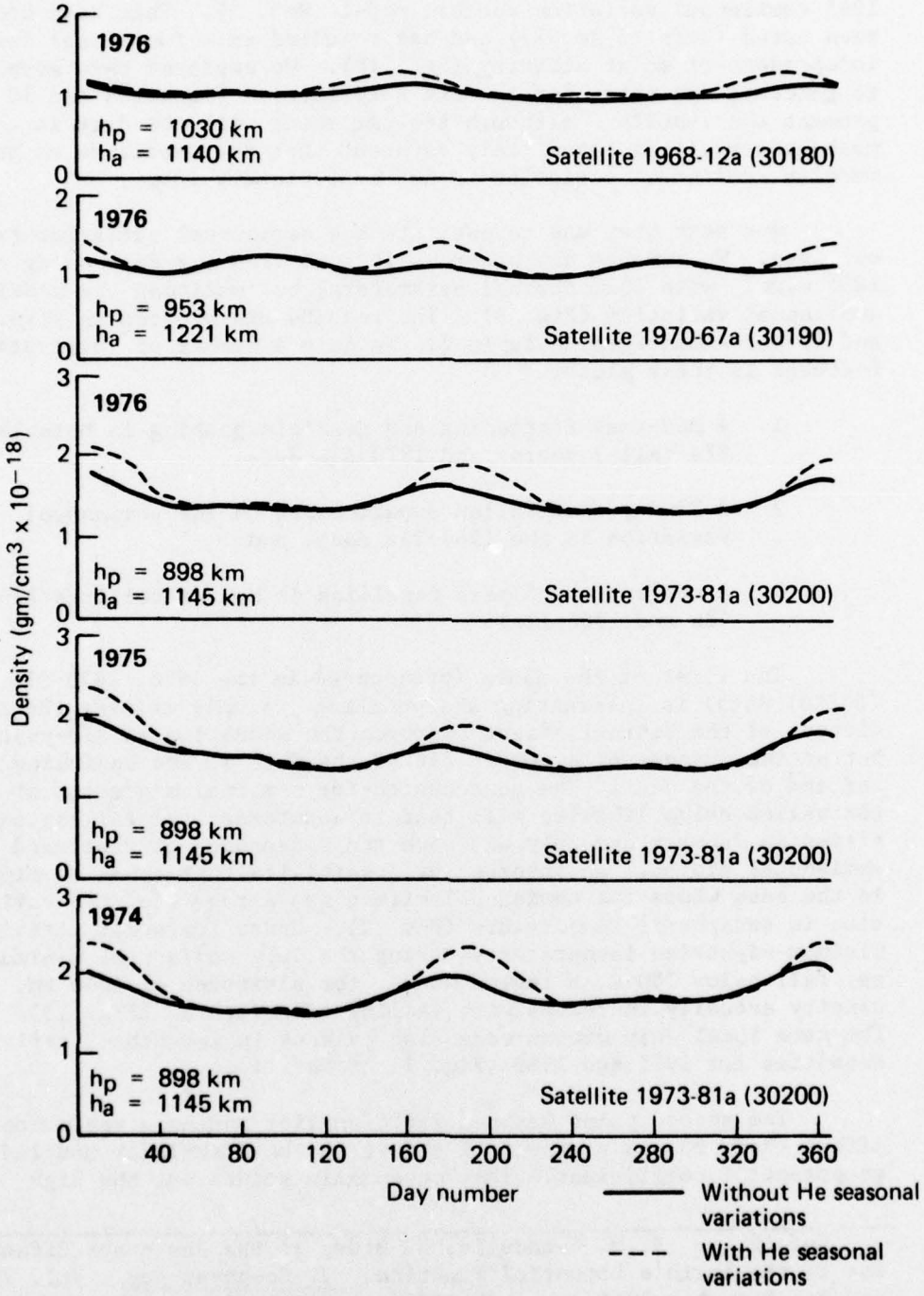

Fig. 8 Mean Modeled Densities versus Time (modeled semiannual variation removed; various satellites)

Figures 6 and 7 clearly illustrate a needed change to the 1965 semiannual variation Jacchia model (Ref. 2). This need had been noted (Refs. 3 and 17) and has resulted in a functional form independent of solar activity (Ref. 18). We employed this model to generate densities for the six satellites. Figures 9 and 10 present the results. Although the agreement with the data is much better, it is immediately apparent that the amplitude of the modeled semiannual variation is not sufficiently large.

Our next step was to estimate the semiannual variation from our data. We removed all other variations from our data using the 1965 model (with 1971 diurnal parameters) but omitting the modeled semiannual variation (Fig. 8). The results are plotted in Figs. 11 and 12 and summarized in Table 2. We note a number of interesting features in these plots:

1. A mid-year flattening and possible peaking in both 1973-81a (all 3 years) and 1970-67a data,

2. A 28-day oscillation superimposed on the semiannual variation in the 1967-34a data, and

3. A suggestion of peak densities in May (satellites 1967-48a and 1968-12a).

The first of the above (pronounced in the 1976, 1973-81a (30200) data) is interesting and puzzling. Simply raising the amplitude of the diurnal effect improves the situation in mid-year but at the expense of a poorer fit of the data at the beginning and end of the year. The unaccounted-for seasonal migration of the helium bulge likewise will tend to counteract the falling densities in January and July and give the appearance of flattened semiannual minima. An interesting possibility that comes to mind is the case where the semiannual effect was a result of the variation in exospheric temperature (Ref. 2). Under low solar activity, minimum nighttime temperatures during the July semiannual minimum may fall below 700 K, a region where, for altitudes of 1000 km, density actually increases with falling temperatures (Fig. 13). The same local July minima were also evident in the Echo-2 derived densities for 1965 and 1966 (Fig. 11 of Ref. 4).

The second point was mentioned earlier and is a resonance effect (Ref. 23) as a result of errors in the 27th-order modeled geopotential coefficient. This once again points out the high

---

Ref. 2. S. M. Yionoulis, "A Study of the Resonance Effects Due to the Earth's Potential Function," J. Geophys. Res., Vol. 70, No. 24, December 1965, pp. 5991-5996, and Vol. 71, No. 4, January 1966, pp. 1289-1291.

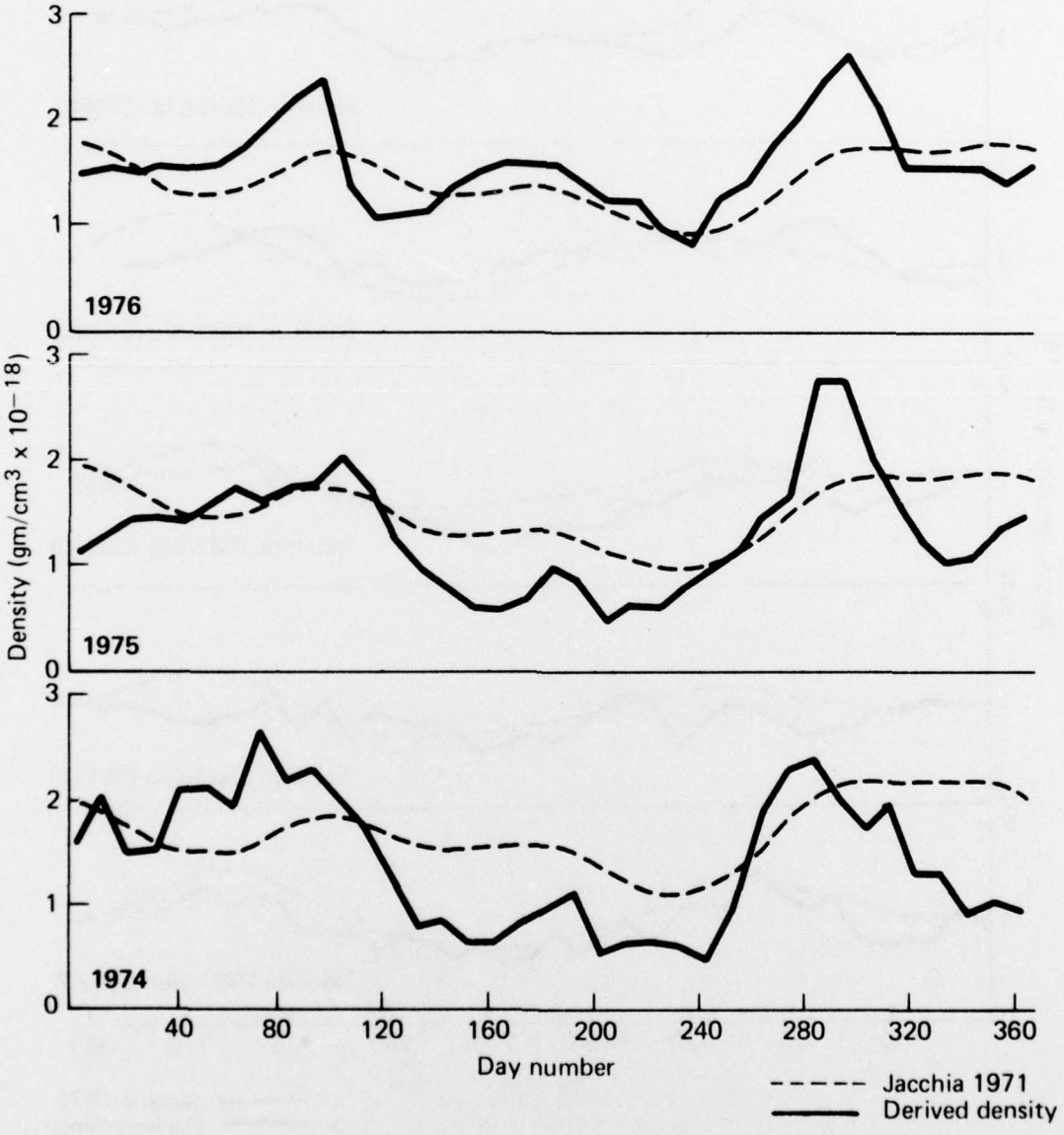

Fig. 9 Mean Atmospheric Density versus Time (modified model; from Satellite 1973-81a (30200) data)

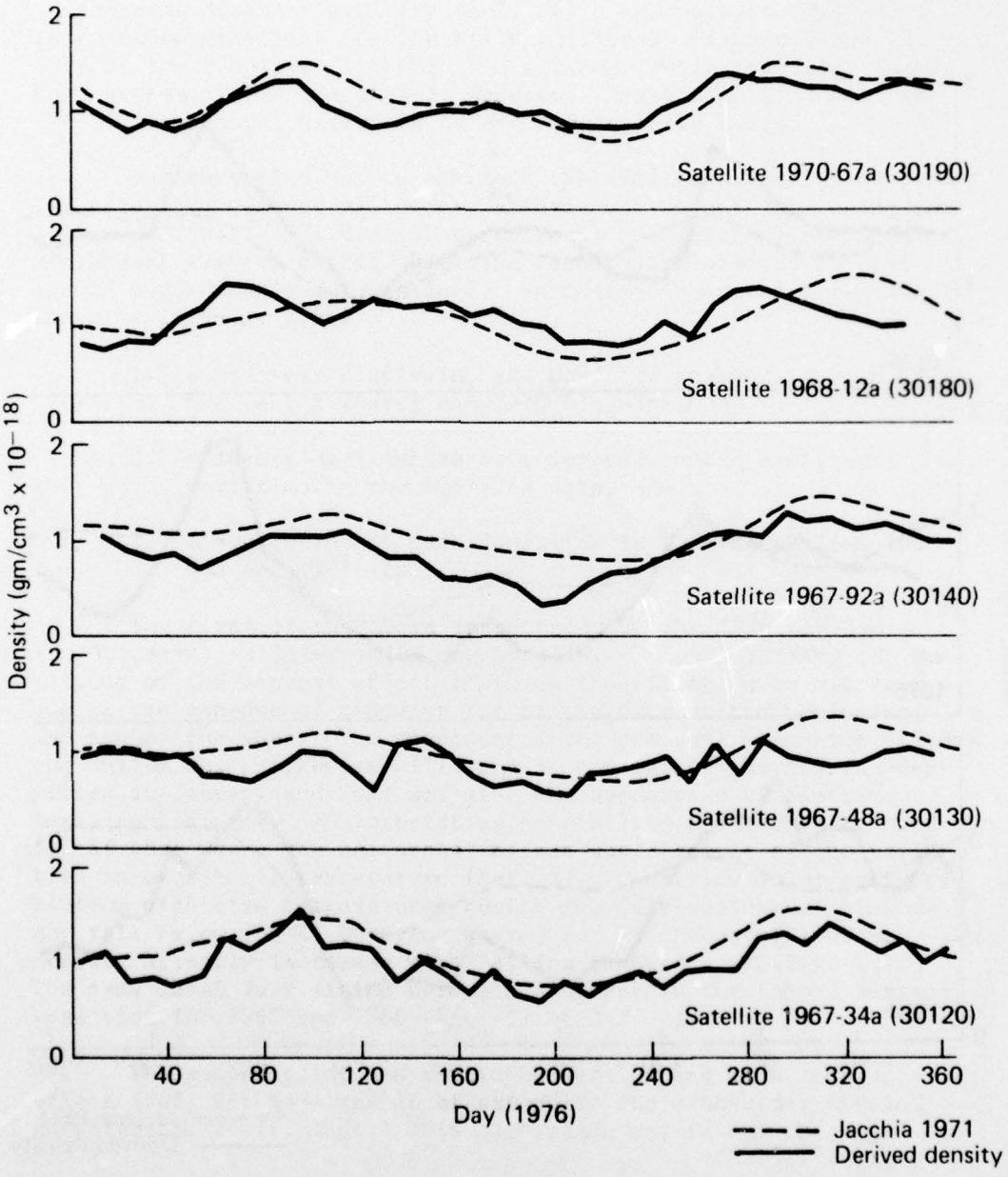

Fig. 10 Mean Atmospheric Density versus Time (modified model; various satellites)

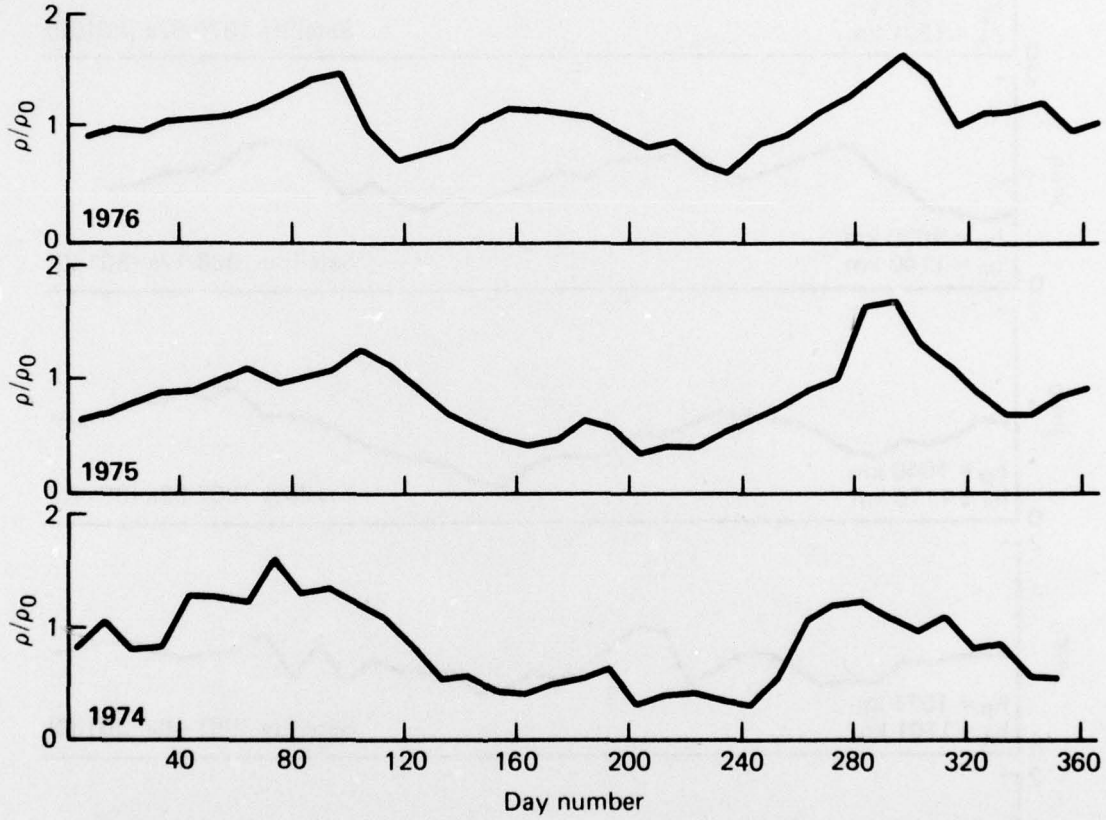

h_p = 898 km
h_a = 1145 km

ρ – Mean density derived from NNSS data
ρ_0 – Modeled mean density with semiannual variation removed

Fig. 11 Semiannual Variation in Density versus Time (derived from Satellite 1973-81a (30200) data)

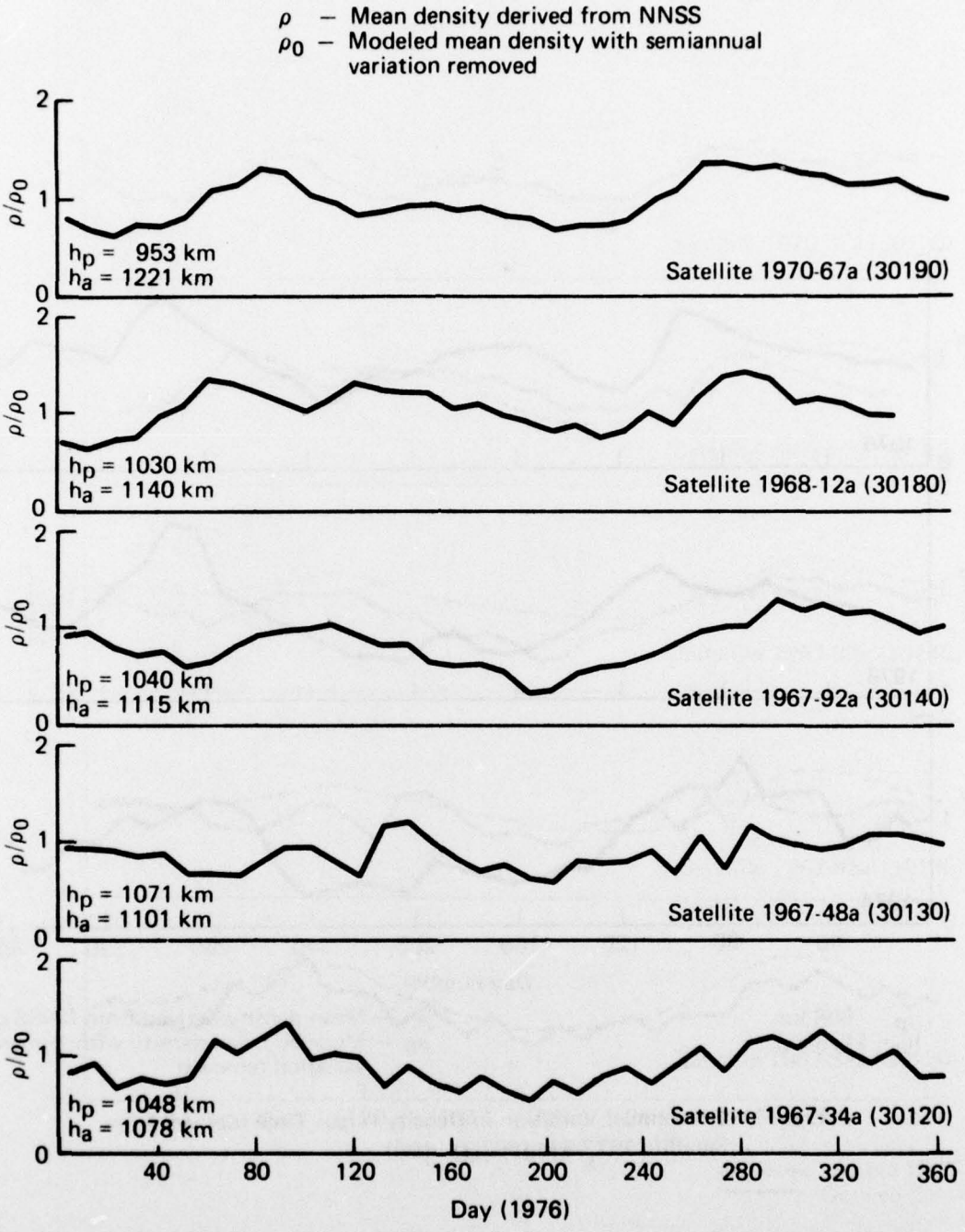

Fig. 12 Semiannual Variation in Density versus Time (derived from data from various satellites)

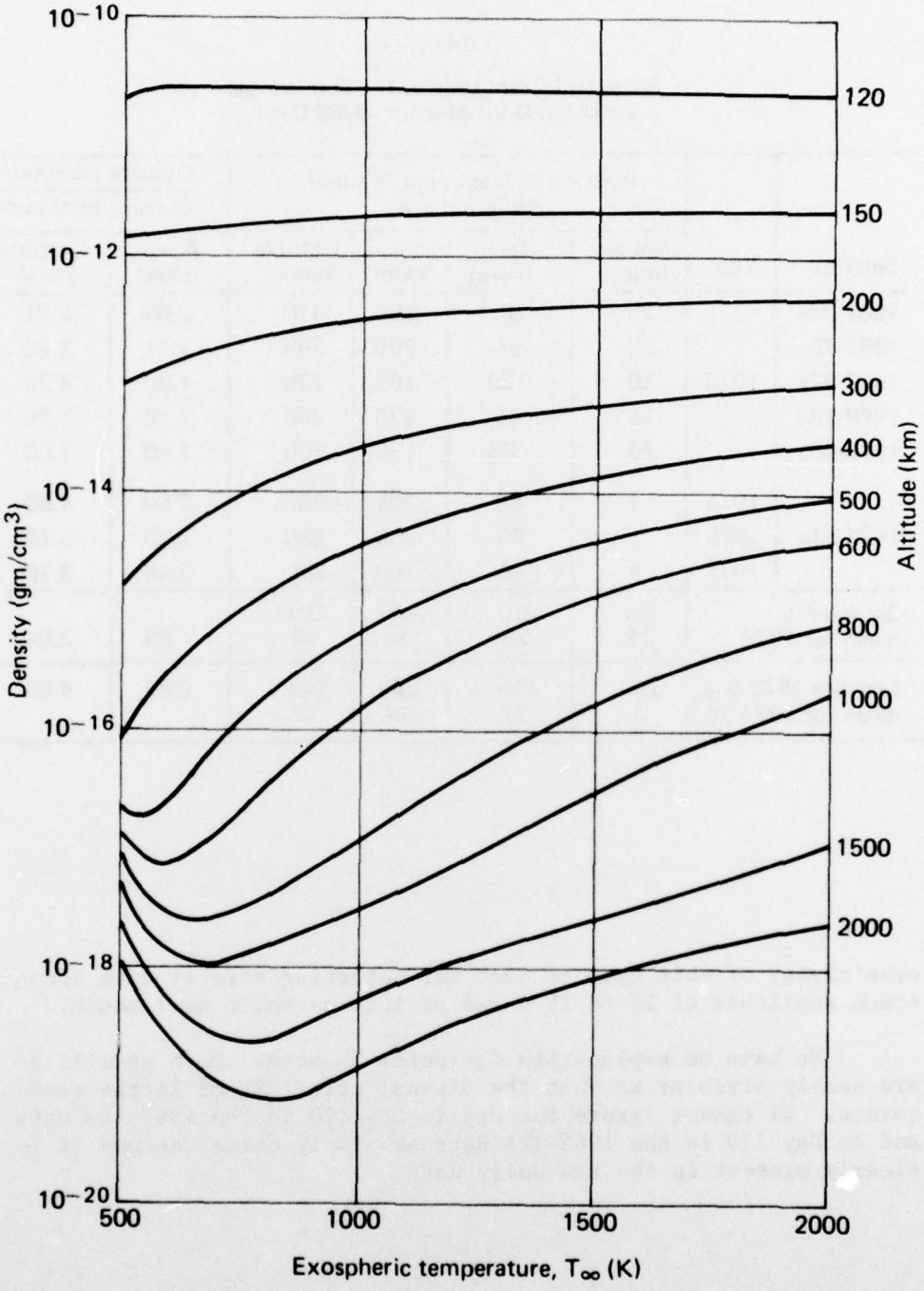

Fig. 13 Dependence of Atmospheric Density on Exospheric Temperature at Different Heights (reproduced from Ref. 18)

Table 2

Phase and Amplitude of the Semiannual Variation Derived from NNSS Data

Satellite	Year	Position of Maximum/Minimun (day number)				Density maximum / Density minimum	
		January (min)	April (max)	July (min)	October (max)	April (max)	October (max)
1967-34a		25	90	190	310	2.03	2.31
1967-48a		60	95	200	285	1.41	2.20
1967-92a	1976	30	100	195	295	1.60	4.20
1968-12a		15	65	220	280	2.10	1.75
1970-67a		20	85	190	290	1.40	1.60
	1974	1	80	205	290	2.60	4.80
1973-81a	1975	1	90	205	290	2.80	5.70
	1976	1	90	180	295	2.46	3.16
Six-satellite mean for 1976		Jan 24	Mar 28	July 14	Oct 19	1.83	2.54
Satellite 1973-81a mean for 1974-76		Jan 1	Mar 27	July 14	Oct 17	2.62	4.55

sensitivity of this type of data for detecting effects with along-track amplitude of 10 to 15 m and periods as short as 1 month.

We have no explanation for point 3 above. Both satellites are nearly circular so that the diurnal effect is of little consequence. We cannot ignore the dip in Day 120 in the 1967-48a data and on Day 110 in the 1968-12a data as simply noise because it is clearly present in the raw daily data.

REFERENCES

1. H. D. Black, R. E. Jenkins, and L. L. Pryor, "The Transit System, 1975," APL/JHU TG 1305, December 1976 (also presented at the 56th Annual American Geophysical Union Meeting 16-20 June 1975).

2. L. G. Jacchia, "Static Diffusion Models of the Upper Atmosphere with Empirical Temperature Profiles," Smithsonian Contribution to Astrophysics, Vol. 8, No. 9, 1965.

3. G. E. Cook and D. W. Scott, "Exospheric Densities Near Solar Minimum Derived from the Orbit of Echo-2," Planet. Space Sci., Vol. 14, 1966, pp. 1149-1165.

4. G. E. Cook and D. W. Scott, "Variations in Exospheric Density at Heights Near 1100 km, Derived from Satellite Orbits," Planet. Space Sci., Vol. 15, 1967, pp. 1933-1956.

5. G. E. Cook and D. W. Scott, "The Semi-Annual Variation on Air Density at Height of 1100 km from 1964 to 1967," Planet. Space Sci., Vol. 17, 1969, pp. 107-119.

6. G. E. Cook, "The Large Semi-Annual Variation in Exospheric Density: A Possible Explanation," Planet. Space Sci., Vol. 15, 1967, pp. 627-632.

7. H. D. Black, "Position Determination Using the Transit System," International Geodetic Symposium on Satellite Doppler Positioning, Las Cruces, NM, 12-14 October 1976.

8. W. H. Guier, "Geodetic Problems and Satellite Orbits," Lectures in Applied Mathematics, Vol. 6, Space Mathematics, Part II, American Mathematical Society, 1966.

9. S. M. Yionoulis, "Determination of Coefficients Associated with the Geopotential Harmonics of Order Thirteen," J. Geophys. Res., Vol. 71, No. 6, March 1966, p. 1768.

10. A. Eisner, "Atmospheric Density Studies," APL/JHU TG 951, December 1967.

11. V. L. Pisacane, B. B. Holland, and H. D. Black, "Recent (1973) Improvements in the Navy Navigation Satellite System," Navigation, Vol. 20, No. 3, Fall 1973, pp. 224-229.

12. H. S. Hopfield, "Two-Quartic Tropospheric Refractivity Profile for Correcting Satellite Data," J. Geophys. Res., Vol. 74, No. 18, August 1969, pp. 4487-4499.

13. S. M. Yionoulis, "Algorithm to Compute Tropospheric Refraction Effects on Range Measurements," J. Geophys. Res., Vol. 75, No. 36, 20 December 1970, pp. 7636-7637.

14. I. Harris and W. Priester, "Theoretical Models for the Solar-Cycle Variation of the Upper Atmosphere," J. Geophys. Res., Vol. 67, No. 12, November 1962, pp. 4585-4591.

15. H. D. Black, "Doppler Tracking of Near-Earth Satellites," APL/JHU TG 1031, 1968.

16. T. O. Seppelin, "The Department of Defense World Geodetic System 1972," The Canadian Surveyor, Vol. 28, No. 5, Ottawa, Canada, December 1974, pp. 496-506.

17. G. E. Cook, "The Semi-Annual Variation in the Upper Atmosphere: A Review," Ann. de Geophys., Vol. 25, 1969, pp. 451-469.

18. L. G. Jacchia, "Revised Static Models of the Thermosphere and Exosphere with Empirical Temperature Profiles," Smithsonian Astrophysical Observatory Special Report 332, May 1971.

19. A. E. Hedin, H. G. Mayr, C. A. Reber, and N. W. Spencer, "Empirical Model of Global Thermospheric Temperature and Composition Based on Data from OGO-6, Quadrapole Mass Spectrometer," J. Geophys. Res., Vol. 70, No. 1, 1975, pp. 215-225.

20. V. Von Zahn, W. Köehnleon, K. H. Fricke, V. Laux, H. Trinds, and H. Volland, "ESRO 4 Model of Global Thermospheric Composition and Temperatures During Times of Low Solar Activity," Geophys. Res. Lett., Vol. 4, No. 1, January 1977, pp. 34-36.

21. G. M. Keating and E. J. Prior, "The Winter Helium Bulge," Space Res., Vol. 8, 1968, pp. 982-992.

22. H. G. Mayr and H. Volland, "Theoretical Model for the Latitude Dependence of the Thermospheric Annual and Semi-Annual Variations," J. Geophys. Res., Vol. 77, No. 34, 1972, pp. 6774-6790.

23. S. M. Yionoulis, "A Study of the Resonance Effects Due to the Earth's Potential Function," J. Geophys. Res., Vol. 70, No. 24, December 1965, pp. 5991-5996, and Vol. 71, No. 4, January 1966, pp. 1289-1291.

Appendix A

DERIVATION OF $A_1 - \delta\rho$ RELATIONSHIP

Using a first-order perturbation theory and ignoring eccentricity effects (Ref. 8), the equations of motion governing the propagation of satellite orbit errors can be written as

$$\dot{H} - 3nH - 2n\dot{L} = F_H \qquad \text{altitude} \qquad \text{(A-1a)}$$

$$\ddot{L} - 2n\dot{H} = F_L \qquad \text{along-track} \qquad \text{(A-1b)}$$

$$\ddot{C} + n^2 C = F_C \qquad \text{cross-track,} \qquad \text{(A-1c)}$$

where H, L, and C are components of the satellite position error resolved (a) in the direction of the satellite radius vector, (b) in the direction of the satellite velocity (along-track), and (c) in the direction of the angular momentrum vector (cross-track), respectively. Errors in the forces acting on the satellite in these three directions are given by F_H, F_L, and F_C. The symbol n is the mean motion of the satellite. Dots denote derivatives with respect to time.

The current knowledge of the geopotential dictates that the major error source in predicting satellite orbits is in the drag force model. A mean error in the modeled drag force is equivalent to a constant force acting in the along-track direction of the satellite's motion (i.e., $F_L = \delta F_d$ = constant). The motion to Eq. A-1 for this constant force is given by

$$H = \frac{2}{3} B_1 + \frac{1}{2} B_2 \sin n(t - t_0) - \frac{1}{2} B_3 \cos n(t - t_0) + \frac{2\,\delta F_d}{n} (t - t_0) \qquad \text{(A-2a)}$$

$$L = B_0 + B_1 n(t - t_0) + B_2 \cos n(t - t_0) + B_3 \sin n(t - t_0) + B_3 \sin n(t - t_0) - \frac{3}{2} F_d (t - t_0)^2 \qquad \text{(A-2b)}$$

$$C = B_4 \cos n(t - t_0) + B_5 \sin n(t - t_0) \, . \qquad \text{(A-2c)}$$

The $B_i (i=0,\ldots 5)$ are the constants of integration and reflect the effects of initial condition errors at $t = t_0$.

From Eq. A-2 we see that the major effect of a mean error in the atmospheric drag-force model is to cause a quadratic growth in the satellite's along-track error. It is also clear that in determining corrections to the initial condition parameters, B_0 and B_1 will be the most sensitive to the F_d error. The remaining parameters are more sensitive to orbital frequency errors.

To estimate the contribution of δF_d to the B_0 and B_1 parameters we can simplify the problem by (a) minimizing only the L residuals and (b) using only the B_0 and B_1 parameters in the theoretical model. Thus we minimize the function

$$F = \int_{t_0}^{t_2} (L^T - L^E)^2 \, dt \qquad \text{(A-3)}$$

with respect to B_0 and B_1 where

$$L^T = B_0 + B_1 \, n(t - t_0) \qquad \text{(A-4)}$$

$$L^E = -\frac{3}{2} \delta F_d (t - t_0)^2 \qquad \text{(A-5)}$$

(cf Eq. A-2b) and t_0 and t_2 are the beginning and ending times, respectively, associated with the fitting (or "tracking") span.

The least-squares solution for B_0 and B_1 is found to be

$$B_0 = \frac{1}{4} (t_2 - t_0)^2 F_d \qquad \text{(A-6a)}$$

$$B_1 = -\frac{3}{2} (t_2 - t_0) \frac{F_d}{n} \, . \qquad \text{(A-6b)}$$

Thus the residuals, after tracking, are given by

$$L^R = \frac{3}{2}\,\delta F_d \left[\frac{1}{6}\,(t_2 - t_1)^2 - (t_2 - t_1)(t - t_0) + (t - t_0)^2\right] \quad \text{(A-7)}$$

and are shown in Fig. A-1. The next fitting interval covers the time span from t_1 to t_3 and the residuals to be minimized are given by Eq. A-7. The theoretical model used to fit to these residuals is again given by

$$L^T = A_0 + A_1\, n(t - t_1)\ , \quad \text{(A-8)}$$

where the epoch is now at t_1. The solution obtained for A_0 and A_1 is

$$A_0 = \frac{3}{2}\,[-(t_2 - t_0) + (t_1 - t_0)]\,(t_1 - t_0)\,\delta F_d \quad \text{(A-9a)}$$

$$A_1 = 3(t_1 - t_0)\,\frac{\delta F_d}{n}\ . \quad \text{(A-9b)}$$

Equation A-9b gives the desired dependence of the A_1 initial-condition parameter with respect to a mean drag-force error.

The atmospheric drag-force acting on the satellite is modeled as

$$F_d = -\frac{1}{2}\,C_d\,\frac{A}{m}\,V^2\,\rho\ , \quad \text{(A-10)}$$

where

C_d = coefficient of drag,

$\frac{A}{m}$ = area-to-mass ratio of the satellite,

V = satellite velocity relative to the atmosphere, and

ρ = atmospheric density.

The atmospheric density is computed using a modified Jacchia model (Ref. 10). From Eq. A-10 we then relate δF_d to a mean error in the computed density, $\delta\rho$:

$$F_d = -\frac{1}{2} C_d \frac{A}{m} V^2 \delta\rho \ . \qquad \text{(A-11)}$$

Substituting Eq. A-11 into Eq. A-9b and solving for $\delta\rho$ yields

$$\delta\rho = -\frac{2}{3}\left[\frac{n}{C_d \frac{A}{m} V^2 (t_1 - t_0)}\right] A_1 \qquad \text{(A-12)}$$

Equation A-12 is the formula used to convert the A_1 data into mean density measurements.

The A_1 parameter can also be expressed as a change in the satellite's semi-major axis, a, at $t = t_1$ via

$$A_1 = -\frac{3}{2} \delta a \ . \qquad \text{(A-13)}$$

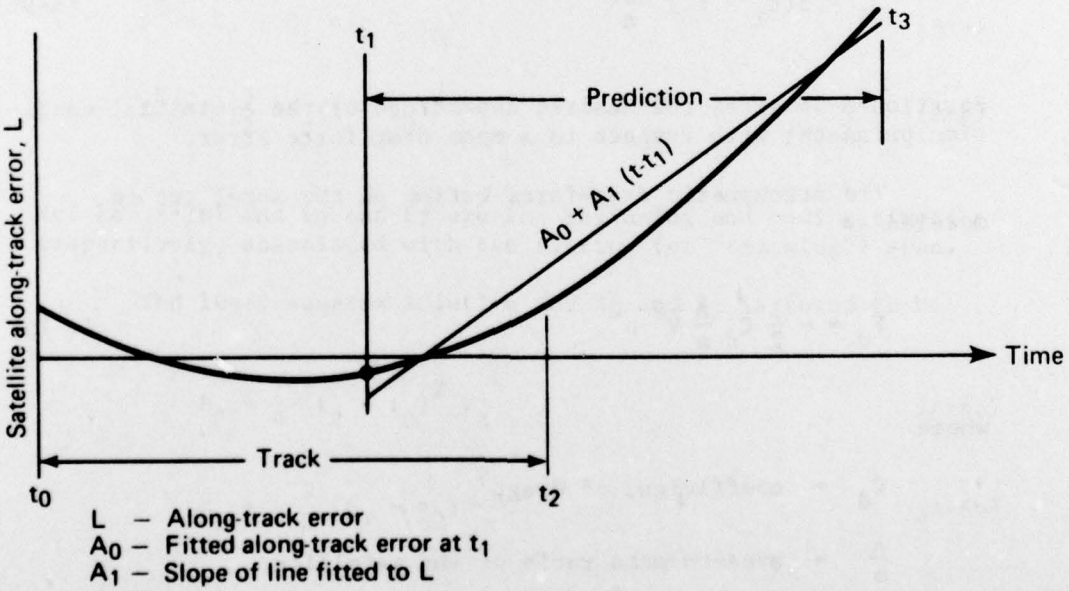

Fig. A-1 Satellite Along-Track Errors Induced by Drag

GLOSSARY

Along-Track Error

The difference between an a priori computed and a least-squares estimated satellite position is resolved in three orthogonal directions. One of these directions lies in the direction of the satellite velocity vector at a particular instant. The corresponding position error component is called "along-track."

APL 4.5 Geopotential Model

A representation of the geopotential (gravity field) as a 16th order/degree Legendre polynomial expansion. This model was developed at APL in 1966 and has been made obsolete by more accurate representation.

NNSS — Navy Navigation Satellite System

Frequently called the Transit System. The system consists of five polar orbiting satellites, all roughly at 1000-km altitude, a network of four tracking sites (all in the USA), a computation center in California, and an injection station to transmit ephemeris data to the satellite.

Resonant Geopotential Effects

If the satellite nodal period is (close to) an integral submultiple of the sidereal day then small errors in a corresponding sectorial harmonic can cause large satellite position errors.

WGS-72

The World Geodetic System 1972 is a representation of the geopotential developed by the Department of Defense in 1972 (Ref. 16).

INITIAL DISTRIBUTION EXTERNAL TO THE APPLIED PHYSICS LABORATORY*

The work reported in TG 1314 was done under Navy Contract N00017-72-C-4401. This work is related to Task S1LO, which is supported by SP-243.

ORGANIZATION	LOCATION	ATTENTION	No. of Copies
DEPARTMENT OF DEFENSE			
DMA	Washington, DC	B. Bowman (52420)	1
DDC	Alexandria, VA		12
Department of the Navy			
NAVSEA	Washington, DC	SEA-09G3	2
NAVAIR	Washington, DC	AIR-50174	2
NAVASTROGRU	Pt.Mugu, CA	CO	1
		L. E. Campbell	1
		R. R. Payne	1
		T. Smith	1
		M. Crawford	1
		G. Kennedy	1
SSPO	Washington, DC	SP-24	1
		SP-243 (LCDR Tomajczyk)	1
		SP-2431 (J. Hoskins)	1
OTHER ORGANIZATIONS			
Smithsonian Astrophysical Observatory	Cambridge, MA	L. Jacchia	1
Royal Aircraft Establishment	Farnborough Hants, England	D. King-Hele	1

Requests for copies of this report from DoD activities and contractors should be directed to DDC, Cameron Station, Alexandria, Virginia 22314 using DDC Form 1 and, if necessary, DDC Form 55.

*Initial distribution of this document within the Applied Physics Laboratory has been made in accordance with a list on file in the APL Technical Publications Group.